Products of the Self-Reaction of HCO Radicals: Theoretical Kinetics Studies

V. Saheb* and A. Nazari

Department of Chemistry, Shahid Bahonar University of Kerman, Kerman 76169-14111, Iran
(Received 20 September 2018, Accepted 29 November 2018)

The self-reaction mechanism of the HCO radicals is investigated using high-level quantum-chemical methods including M05-2X, CCSD, CCSD(T) and CRCC(2,3). Next, the rate coefficients for several product channels as a function of pressure and temperature are computed by employing statistical rate theories. Four important product channels are predicted to be $CO + CO + H_2$, $HCOH + OH$, *cis*-$(HCO)_2$ and *trans*-$(CHO)_2$. It is found that the bimolecular rate coefficients for the formation of *cis*-$(HCO)_2$ and *trans*-$(CHO)_2$ are strongly pressure-dependent. The rate coefficients for the product channels $CO + CO + H_2$ and $HCOH + OH$ are predicted to be slightly pressure-dependent. At lower pressures and higher temperatures, the products $CO + CO + H_2$ and $HCOH + OH$ are dominant, while at higher pressures and lower temperatures, *cis*-$(HCO)_2$ and *trans*-$(CHO)_2$ formation becomes important.

Keywords: Formyl radical, HCO, Self-reaction, Quantum chemical methods, Theoretical, Kinetic studies

INTRODUCTION

Formyl radical (HCO) has received considerable experimental and theoretical studies because of its importance in combustion chemistry of hydrocarbons [1-9]. HCO radicals are produced in the middle of the oxidation pathway of hydrocarbons [1]. The C-H bond dissociation energy in HCO is relatively low (about 58.3 kJ mol^{-1}) [2] so that it rapidly dissociates to H + CO or undergoes bimolecular reactions with other radical species produced during the combustion process. As a consequence, many studies are devoted to characterize the molecular properties of HCO radical [3-6] and its unimolecular decomposition reaction [7,8]. The bimolecular reactions of HCO radical with radicals such as H, NO and NO_2 have also been investigated [9].

One important process in the degradation of HCO radicals in combustion reaction is the self-reaction of HCO radicals. To date, many experimental studies are reported in the literature on the kinetics of the HCO + HCO reaction, and $CO + CO + H_2$, $CH_2O + CO$ and $(HCO)_2$ are introduced

─────────

*Corresponding authors. E-mail: vahidsaheb@uk.ac.ir

as the main product channels of the reaction [4,10-19]. A synopsis of the reported data on the kinetics of the title reaction is given in Table 1. It should be mentioned that some research groups have reported $CH_2O + CO$ [4,11-14] as the main product while $CO + CO + H_2$ [10] and $(HCO)_2$ [10,15] are determined as the main product channels by some other researchers. The overall rate coefficients are reported from some laboratories [16-19].

In the present research, the mechanism and kinetics of HCO + HCO reaction is investigated theoretically. High-level quantum chemical methods are used to search various possible product channels. Next, well-tested statistical rate methods are employed to compute the rate coefficients for the formation of different products. The pressure and temperature dependency of the rate coefficients of various product channels are also studied and discussed.

COMPUTATIONAL DETAILS

First, the hybrid meta DFT method M05-2X along MG3S basis set [20,21] is used to locate kinetically important structures involved in the HCO + HCO reaction. Starting from the latter optimized structures, the obtained

Table 1. The Rate Coefficients for Different Product Channels of the Title Reaction Reported by Various Laboratories[a]

| T	A	Ref.[b]
(K)	(cm^3 molecule^{-1} s^{-1})	
$HCO + HCO \rightarrow CO + CO + H_2$		
303-376	3.63×10^{-11}	Quee 1968 [10]
$HCO + HCO \rightarrow CH_2O + CO$		
298	6.31×10^{-11}	Reilly 1978 [4]
300	3.0×10^{-11}	Sarkisov 1984 [12]
298-475	3.35×10^{-11}	Veyret 1984 [13]
295	7.5×10^{-11}	Baggot 1986 [14]
$HCO + HCO \rightarrow (HCO)_2$		
303-376	2.76×10^{-13}	Quee 1968 [10]
298	5.0×10^{-11}	Stoeckel 1985 [15]
$HCO + HCO \rightarrow$ Products		
298	3.0×10^{-11}	Nadtochenko 1979 [16]
298	2.32×10^{-11}	Hochanadel 1980 [17]
298	3.57×10^{-11}	Mulenko 1980 [18]
296	4.48×10^{-11}	Temps 1984 [19]

[a]The activation energy is reported to be zero by all available experimental measurements. [b]The values in the parentheses are the corresponding reference numbers.

geometries are re-optimized by the more sophisticated CCSD/Aug-cc-pVDZ method [22,23]. Higher levels of theory is employed to have more accurate estimations of energies including CCSD(T) and CR-CC(2,3) methods [24,25]. CR-CC(2,3) is a completely re-normalized (CR) coupled cluster (CC) method in which the effects of triply (T) and other higher-than-doubly excited clusters are added to the CCSD method so that the full configuration-interaction energies are recovered. It is demonstrated that CR-CC(2,3) energies are practically as accurate as multi-reference configuration interaction method (MRCI) [26] and the full CC approach with singles, doubles, and triples in the bond-breaking region [24,25]. Augh-cc-pVTZ+2df and Aug-cc-pVQZ basis sets [23] are used along with CCSD(T) method, and Aug-cc-pVTZ basis set is used along with CR-CC(2,3) method. M052-X, CCSD and CCSD(T)

calculations are carried out with the Gaussian 09 package of programs [27]. GAMESS package of programs is employed for computing CR-CC(2,3) calculations [28-30].

In the following section we will show how the chemically-activated intermediates *cis*- and *trans*-$(CHO)_2$ are formed through the C-C bond formation. This intermediates decompose to yield products. The rate constants for the formation of the adducts *cis*- and *trans*-$(CHO)_2$ and the products originating from their decomposition as a function of pressure and temperature, is evaluated by implementing a master equation (ME) formalism [31,32]. There are a complete description of the ME method in the references 31 and 32. Here, only a very brief statement of the method is presented. When a chemically-activated intermediate is appeared during a bimolecular reaction as:

$$R + R' \underset{k_i}{\overset{v_i}{\rightleftarrows}} A^* \overset{k_i'}{\longrightarrow} \text{products}$$
$$\downarrow$$
$$A$$
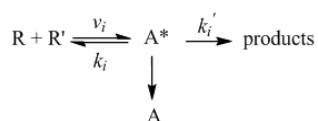
The rate of variation in the population density of the activated adduct with energy E_i, is given by the following equation:

$$\frac{dn_i}{dt} = V_i + \omega \sum_j P_{ij} n_j - \omega n_i(t) - (k_i + k_i') n_i(t) \qquad (1)$$

where n_i is the population density of the adduct, ω is the frequency of molecular collision, P_{ij} is the probability for energy transfer from j to i, k_i, and k_i' are the microcanonical rate coefficients for unimolecular decomposition reaction of the intermediate to reactants and products, respectively. The rate constant for the formation of products is given by

$$k_D = \sum_i k_i' n_i \qquad (2)$$

The rate constant for the formation of the adduct is

$$k_\varepsilon = \sum V_i + \sum_i (k_i + k_i') n_i \qquad (3)$$

The microcanonical rate coefficients, appeared in the Eqs.

(1) to (3), are computed according to the RRKM theory,

$$k(E) = L \frac{Q_1^+}{Q_1} \frac{W(E_{Vr}^+)}{h\rho(E)} \qquad (4)$$

where L is the statistical factor, h is Plank's constant, $W(E_{vr}^+)$ is the sum of active vibrational and rotational states for the transition state, $\rho(E)$ is the density of active quantum states for reactant, Q_1^+ and Q_1 are the partition functions for the adiabatic rotations in the transition state and reactant. As stated, the C-C bonds are formed during the formation of *cis*-$(CHO)_2$ and *trans*-$(CHO)_2$ which are barrierless processes. In order to evaluate the energy-specific rate coefficients of the latter processes, the more sophisticated version of RRKM, variable reaction coordinate transition state theory (VRC-TST) is employed [33-38]. In VRC-TST, sum of quantum states of transition state is computed according to the following convolution integral,

$$W(E_{Vr}^+) = \int_0^{E'} N_V(E' - \varepsilon)\Omega(\varepsilon)d\varepsilon \qquad (5)$$

where $N_V(E' - \varepsilon)$ is the number of states of the conserved modes which have an energy equal to or less than $E' - \varepsilon$, and E' is the accessible energy; *i.e.*, E minus the zero point corrected potential energy minimum at a determined value of reaction coordinate. $\Omega(\varepsilon)d\varepsilon$ is the number of states corresponding to the transitional modes at the given E lying in $(\varepsilon, \varepsilon + d\varepsilon)$. N_V and Ω are computed by the direct-count method and Mont Carlo procedures, respectively. In order to compute Ω, the potential for the interactions of separating moieties is considered as the sum of a bonding potential for the bond breaking and the sum of 6-12 Lennard-Jones potential terms for remaining inter-fragment interactions [37]. The Variflex code, developed by Klippenstein *et al.*, is used to carry out the VRC-TST calculations [38]. In the next section we will how the unimolecular rate coefficients for the anti-HCOH $\rightarrow$ CH_2O isomerization process is computed using SCTST approach [39-41]. In SCTST, the sum of quantum states in Eq. (4), is replaced with the concept of cumulative reaction probabilities, CRP, defined according to the following equation:

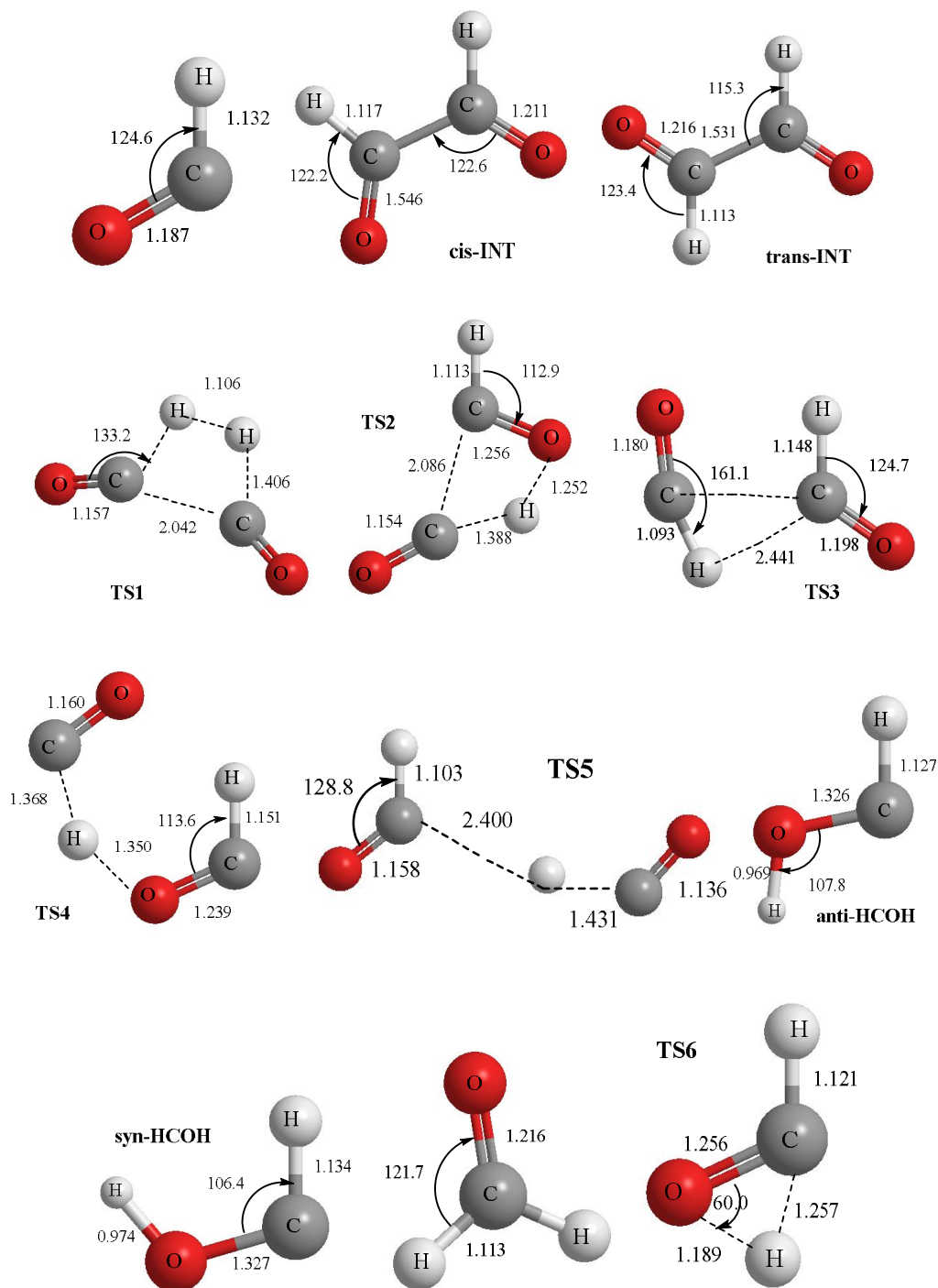$$G_V^\mp(E_V) = \sum_{n_1} \sum_{n_2} \cdots \sum_{n_{F-2}} \sum_{n_{F-1}} P_n(E_V) \qquad (6)$$

here P_n is the semiclassical tunneling probability for n^{th} vibrational quantum state. For a given vibrational state with energy of E, P_n is given by the following equation:

$$P_n(E) = \frac{1}{1 + \exp[2\theta(n,E)]} \tag{7}$$

In this equation, $\theta(n,T)$ is the barrier penetration integral. Considering vibrations of transition state as coupled anharmonic oscillators, $\theta(n,T)$ is computed by a Monte Carlo algorithm [41-42]. SCTST calculations are carried out with MultiWell-2016 Software [44].

RESULTS AND DISCUSSION

Based on the theoretical results obtained in the present research work and the data obtained from experimental studies reported by different laboratories, the mechanism of HCO + HCO reaction can be represented by the following scheme:

$$HCO + HCO \rightarrow cis-(HCO)_2 \xrightarrow{TS1} 2CO + H_2 \qquad R1$$
$$\rightarrow trans-(HCO)_2 \xrightarrow{TS2} anti-HCOH + CO \quad R2$$
$$\xrightarrow{TS3} CH_2O + CO \qquad R3$$
$$HCO + HCO \xrightarrow{TS4} syn-HCOH + CO \qquad R4$$
$$HCO + HCO \xrightarrow{TS5} CH_2O + CO$$

The optimized structures of the molecular species involved in the self-reaction of CHO radical are demonstrated in Fig. 1. The minimum energy path connecting two minima on the PES are followed by the intrinsic reaction coordinate (IRC) calculations [45]. The moments of inertia, vibrational frequencies and z-matrices of the reactant, intermediates and transition states are given as Supporting Information.

In the following, a brief description of the mechanism of the title reaction is presented. The energies are those obtained by the CCSD(T)/Aug-cc-pVQZ method. HCO radicals could undergo an association reaction via a C-C bond to form trans- or cis-(HCO)$_2$ intermediates. Here, these chemically-activated intermediates are called trans-(CHO)$_2$ and cis-(CHO)$_2$. The energies of trans-(CHO)$_2$ and cis-(CHO)$_2$ relative to the reactants are -295.1 kJ mol^{-1} and -276.7 kJ mol^{-1}, respectively. Cis-(CHO)$_2$ is formed due to

the stabilization of the chemically-activated cis-(CHO)$_2$ by collisions to bath-gas molecules. The chemically-activated cis-(CHO)$_2$ can also undergo a unimolecular decomposition reaction to form CO + CO + H$_2$ (R1) via passing over the saddle-point structure TS1. A barrier height of 234.9 kJ mol^{-1} should be surmounted by cis-(CHO)$_2$ in the latter process. CO + CO + H$_2$ is computed to be -308.6 kJ mol^{-1} more stable than the reactants (HCO + HCO). Trans-(CHO)$_2$ could decompose via the four-membered ring TS2 to yield anti-HOCO + CO (R2). The barrier height for trans-(CHO)$_2$ $\rightarrow$ anti-HOCO + CO is calculated to be 251.6 kJ mol^{-1}. Anti-HOCO + CO is -83.1 kJ mol^{-1} more stable than the HCO + HCO. The chemically activated adduct of trans-(CHO)$_2$ may also undergo a unimolecular decomposition via transition state TS3 to give CH$_2$O + CO (R3). The barrier height for the trans-(CHO)$_2$ $\rightarrow$ CH$_2$O + CO is 316.7 kJ mol^{-1} and the relative energy of CH$_2$O + CO is -303.8 kJ mol^{-1}. The potential energy profile of the title reaction is depicted in Fig. 2.

Syn-HCOH + CO and CH$_2$O + CO may also be formed from the HCO radicals via two direct hydrogen abstraction reactions. HCO radicals react via a six-membered ring transition state (TS4) to form syn-HCOH + CO, see Fig. 1. An activation energy of 2.2 kJ mol^{-1} is obtained for the latter process. A hydrogen atom shift occurs from one HCO radical to carbon atom of another HCO via transition-state TS5 to form CH$_2$O + CO. The activation energy for passing through TS5 is 28.1 kJ mol^{-1}. The relative energies calculated by different levels of theory are given in Table 2.

A ME formalism is used to compute the rate constants for the production of cis-(CHO)$_2$, trans-(CHO)$_2$, CO + CO + H$_2$, syn-HCOH + CO, anti-HCOH + CO and CH$_2$O + CO. As mentioned in the previous section, the association processes of the formation of intermediates cis-(CHO)$_2$ and trans-(CHO)$_2$ are barrierless processes. In order to compute the energy-specific rate coefficients of these association processes, the VRC-TST approach is used [33-38]. The vibrational wave numbers and principal moments of inertia for HCO, intermediates and transition-states are provided in Table 1S in Supplemental Information.

Figure 3 demonstrates the pressure-dependency of the predicted bimolecular rate coefficients for the production of cis-(CHO)$_2$ at several temperatures. As seen, the rate coefficients increase as pressure is elevated because of

Fig. 1. The geometries of reactant, intermediates, transition states and products arising from the reaction HCO + HCO, computed at the ccsd/aug-cc-pVDZ level of theory.
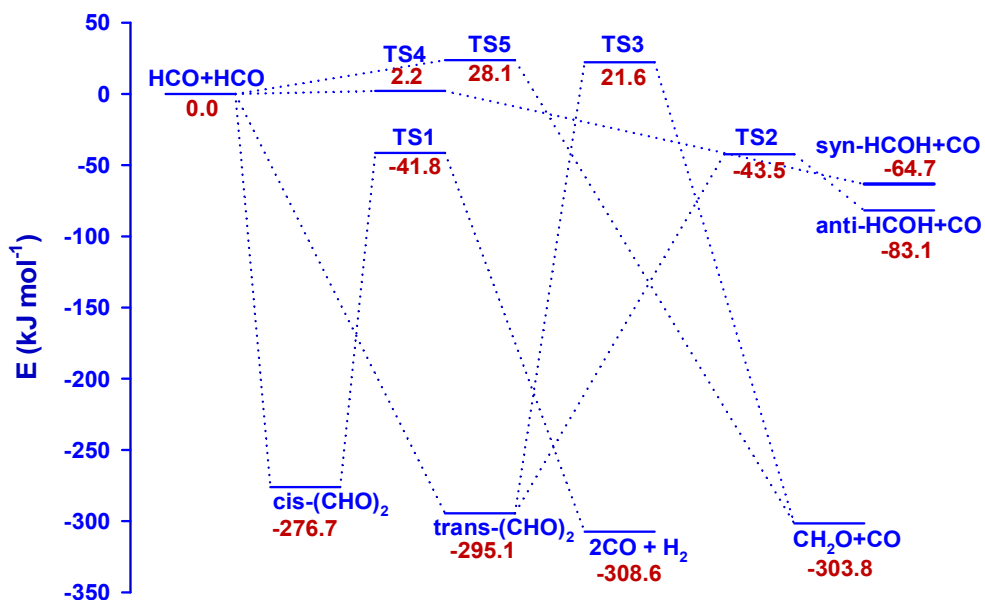
Fig. 2. Relative energies of the stationary points located on the singlet ground-state potential energy surface of the HCO + HCO reaction.

Table 2. The relative energies of the intermediates, transition states and products involved in the HCO + HCO reaction in kJ mol^{-1}

	CCSD(T)/BS1	CCSD(T)/BS2	CRCC(2,3)/BS3
Reactants (2HCO)	0	0	0
cis-(CHO)$_2$	-276.1	-276.7	-261.3
trans-(CHO)$_2$	-294.5	-295.1	-279.1
TS1	-41.4	-41.8	-33.2
TS2	-42.3	-43.5	-32.8
TS3	24.9	21.6	38.1
TS4	1.3	2.2	11.1
TS5	23.8	28.1	41.4
CO + CO + H$_2$ (P1)	-307.4	-308.6	-309.7
anti-HCOH + CO (P2)	-81.7	-83.1	-84.6
CH$_2$O + CO (P3&P5)	-301.6	-303.8	-298.8
syn-HCOH + CO (P4)	-63.23	-64.7	-66.4

*BS1 = Augh-cc-pVTZ+2df. BS2 = Aug-cc-pVQZ. BS3 = Aug-cc-pVTZ.
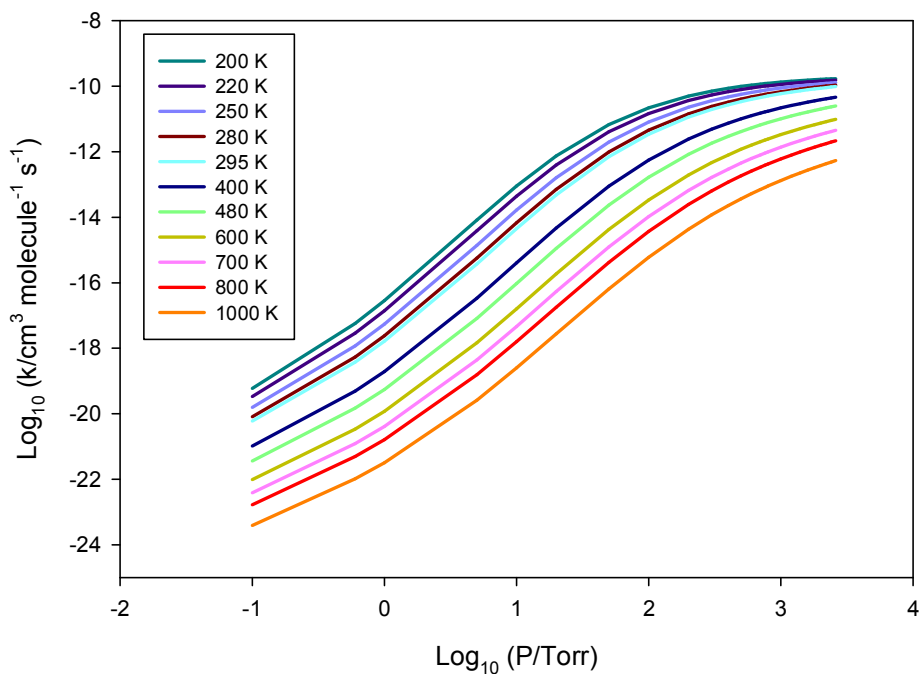
Fig. 3. The computed bimolecular rate constants for the formation of *cis*-$(HCO)_2$ at some selected temperatures in the range of 200-1000 K as a function of pressure.
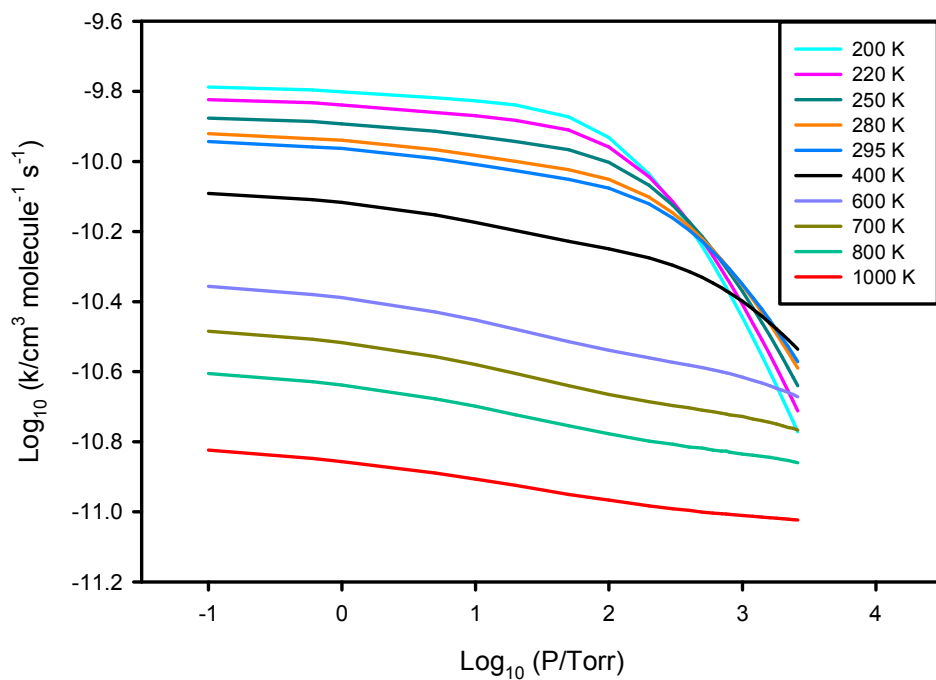
Fig. 4. The computed bimolecular rate constants for the formation of $CO + CO + H_2$ at some selected temperatures in the range of 200-1000 K as a function of pressure.

increasing the number of molecular collisions with increase of pressure. More collisions cause more deactivation. The rate coefficients are predicted to decrease with temperature elevation. There are two important reasons for the decrease of the rate coefficients. The main reason is that the microcanonical rate coefficients for the association entrance channel HCO + HCO decrease as the molecular energies increase. This is a well-known fact that the position of the bottle-neck of the association processes move to shorter inter-fragment distances with increase of molecular energies. The second reason is that the chemically-activated cis-$(CHO)_2$, formed from the association process HCO + HCO, dissociates faster at higher energies. Here, the barrier height for dissociation of cis-$(CHO)_2$ to CO + CO + H_2 is lower than that for its dissociation back to reactants. Therefore, it is predicted that cis-$(CHO)_2$ will dissociates dominantly to CO + CO + H_2.

Figure 4 shows the pressure-dependency of the predicted bimolecular rate coefficients for the product channel CO + CO + H_2 at several temperatures. The rate constants are predicted to be pressure-independent at temperatures higher than about 400 K. At lower temperatures, the computed rate coefficients slightly decline with pressure increase. Inspection of the absolute values of the rate coefficients presented in Figs. 3 and 4 reveals that once the activated adduct of cis-$(CHO)_2$ is formed, it dissociates more rapidly to CO + CO + H_2 than it is deactivated by molecular collisions. The calculated rate constants as a function of temperature at some selected pressures for the formation of CO + CO + H_2 are also demonstrated in Fig. 5. The available experimental data reported in the literature are also given for the purpose of comparison. To date, there is only one report on the product channel CO + CO + H_2. As seen, it seems that the present calculations slightly overestimates the rate coefficients in comparison with this single experimental data. However, if the absolute values of the computed rate coefficients are considered carefully, it is understood that there is a good agreement between the present theoretical results and experimental data.

The computed rate constants for the formation of cis-$(CHO)_2$ along with those for CO + CO + H_2 are provided in Fig. 1S in Supporting Information for the purpose of comparison. These theoretical results show that CO + CO + H_2 is the dominant product channel at low pressures and higher temperatures. As abovementioned, the reason is that the deactivation of the chemically-activated adduct of cis-$(CHO)_2$ becomes significant as pressure increases. For example, at 200 K, the product channel CO + CO + H_2 is dominant at pressures below about 10 Torr while at 600 K, the product channel CO + CO + H_2 becomes dominant at pressures below about 1000 Torr.

As shown by the PES of the HCO + HCO reaction, two products originating from $trans$-$(CHO)_2$ are anti-HOCO + CO and CH_2O + CO. Figure 6 demonstrates the predicted pressure-dependency of the rate coefficients for the product channel $trans$-$(CHO)_2$ at some selected temperatures. Essentially, similar results as for the formation of cis-$(CHO)_2$ are obtained. The computed rate constants at several temperatures for the product channel anti-HOCO + CO as a function of pressure are shown Fig. 7. The computed rate constants are slightly pressure dependent at low temperatures. It is found that the rate coefficients computed for the product CH_2O + CO originated from $trans$-$(CHO)_2$ is much smaller than those for anti-HOCO + CO. The rate coefficients computed for the production of CH_2O + CO are found to be pressure-independent and are fitted to the rate constants expression $k_3 = 6.76 \times 10^{-7} \exp(-5.92 \text{ kJ mol}^{-1}/RT) \text{ cm}^3 \text{ molecule}^{-1} \text{ s}^{-1}$.

It is worth mentioning here that in all experimental measurements, the rate coefficients for the formation of CH_2O + CO (not anti-HCOH + CO) are reported. The PES of the reaction shows that the product channel anti-HCOH + CO (with relative energy of -83.1 kJ mol^{-1}) is relatively exothermic process. The question raised is to what extent the isomerization process anti-HCOH $\rightarrow$ CH_2O occurs in the reaction condition of the present study. In order to address this latter question, the microcanonical unimolecular rate coefficients for the anti-HCOH $\rightarrow$ CH_2O process are computed by using SCTST. The computed barrier height of anti-HCOH $\rightarrow$ CH_2O reaction at the CCSD(T)/Aug-cc-pVQZ level is 127.6 kJ mol^{-1}. The computed values of the rate coefficients at some selected energies are given in Supplemental Information. The unimolecular rate constant at the energy of 83.0 kJ mol^{-1} (the minimum energy released according to the PES during the formation anti-HCOH + CO) is computed to be about 4×10^6 s^{-1}. It should be mentioned here that the reaction would not occur according to the RRKM theory if the
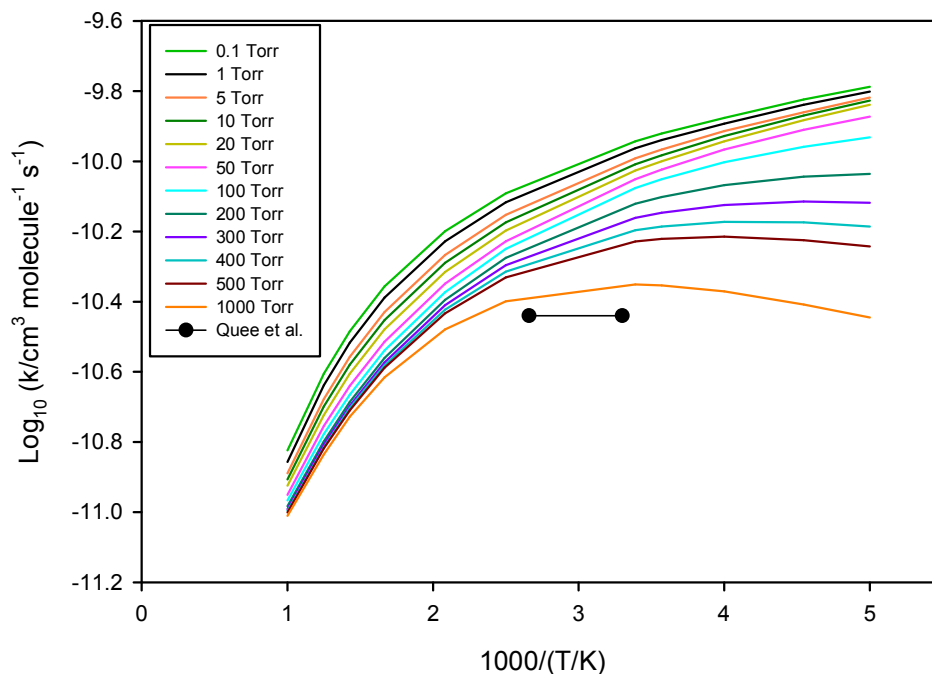
Fig. 5. The computed thermal rate coefficients for the product channels $CO + CO + H_2$ at some selected pressures as a function of temperature. The single experimental data reported by Quee and Thynne (Ref. [10]) are given for the purpose of comparison.
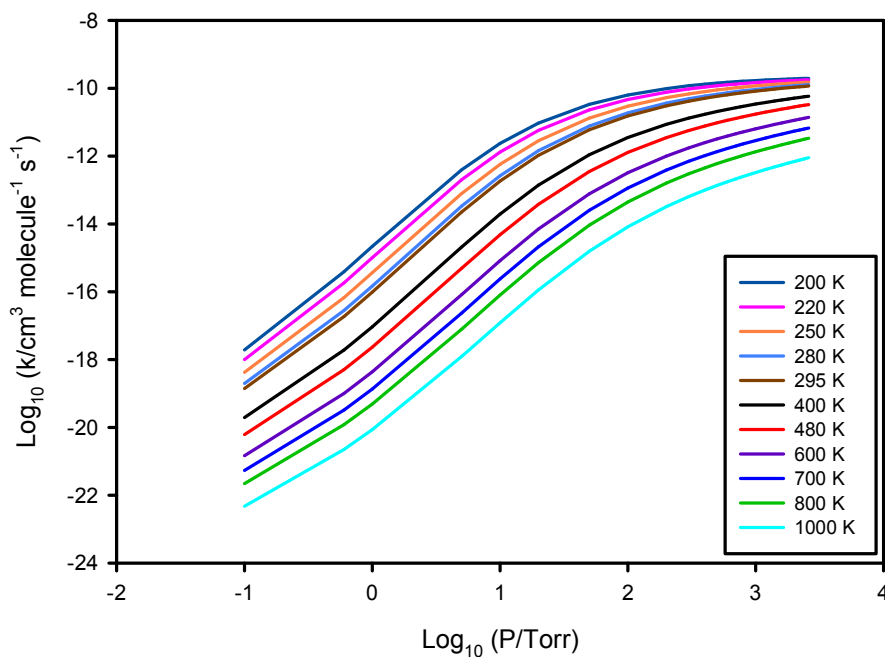

Fig. 6. The computed bimolecular rate constants for the formation of *trans*-$(HCO)_2$ at some selected temperatures in the range of 200-1000 K as a function of pressure.
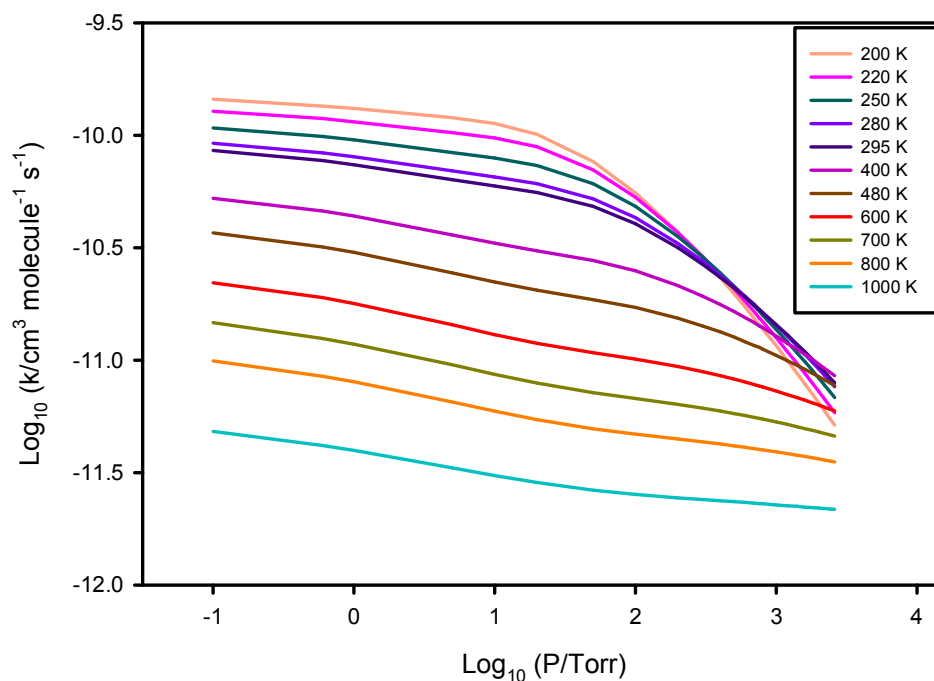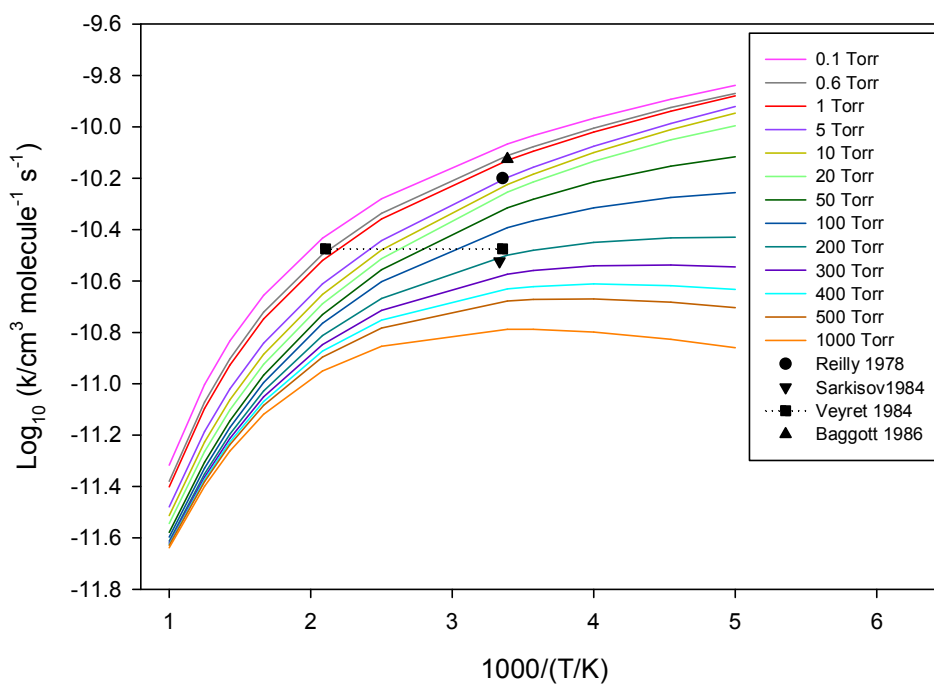
Fig. 7. The computed bimolecular rate constants for the formation of HOCO + CO at some selected temperatures in the range of 200-1000 K as a function of pressure.

Fig. 8. The computed thermal rate coefficients for the product channels HOCO + CO at some selected pressures as a function of temperature. The available experimental data are given for the purpose of comparison.

tunneling effect is neglected. The latter isomerization reaction occurs at energy of 83.0 kJ mol^{-1} only due to the tunnel effect. The computed value at 127.6 kJ mol^{-1} (barrier height of anti-HCOH → CH$_2$O reaction) is computed to be 5×10^{10} s^{-1}. The values of the deactivation rate coefficients are of the order of 10^8-10^{10} s^{-1} over the pressure range 10-1000 Torr. This values show that once the energized anti-HCOH is formed, it undergoes a deactivation process at moderate pressures and temperatures before isomerization to CH$_2$O occurs.

Figure 8 shows the temperature-dependency of the rate coefficients for the formation of anti-HOCO + CO at several pressures. For the purpose of comparison, the reported experimental data for the rate constants of CH$_2$O + CO production are also given in Fig. 8. It can be seen that the theoretically predicted rate constants for the production of anti-HCOH + OH are in accordance with the experimental data. The results presented in Fig. 8 along with the computed microcanonical rate coefficients for the anti-HCOH → CH$_2$O process convince us what is formed during the reaction path R2 is anti-HCOH. The rate coefficients computed for the production of *trans*-(CHO)$_2$ and anti-HOCO + CO are demonstrated in one figure (Fig. 2S) in Supplemental Information. The results show that at low pressures and higher temperatures, anti-HOCO + CO is dominantly produced. The reason is similar to that presented for the reaction path proceeding through *cis*-(CHO)$_2$. Here, due to the relatively low barrier of the *trans*-(CHO)$_2$ → anti-HOCO + CO process, the activated adduct of *trans*-(CHO)$_2$ dissociates rapidly to anti-HOCO + CO before it is deactivated by molecular collisions.

As aforementioned, the reaction HCO + HCO may proceed *via* a six-membered ring saddle-point structure (TS4) leading to syn-HCOH + OH. The product CH$_2$O + CO could also be formed directly *via* TS5. The barrier heights of the latter processes are 2.2 and 28.1 kJ mol^{-1}, respectively. The rate constants of the latter reaction channels are calculated by CTST. The theoretically predicted rate constants are fitted to the expressions $k_4 = 5.0 \times 10^{-22}$ ($T^{2.85}$) exp(800/T) and $k_5 = 2 \times 10^{-25}$ ($T^{4.14}$) exp(-1641/T), respectively. It should be mentioned that the rates of the latter reaction paths are much slower than those for the formation of *cis*-(CHO)$_2$, *trans*-(CHO)$_2$ and anti-HCOH + OH. It is concluded from the above results that the product

CO + CO + H$_2$ and anti-HCOH + OH, respectively, originating from *cis*-(CHO)$_2$ and *trans*-(CHO)$_2$ are the most important products of the HCO + HCO reaction. The present calculations suggest that the molecules appearing in experiments with molecular formula CH$_2$O is dominantly anti-HCOH not formaldehyde. It is noteworthy to mention that all the experimental data reported to date are based on the measurements of transient ultraviolet absorption spectrum for HCO radicals. The present theoretical investigation encourages further experimental studies on the title reaction.

CONCLUSIONS

The mechanism of the self-reaction of HCO is investigated by the high-level quantum-chemical calculations. Next, the bimolecular rate constants for the formation of important products are computed by statistical rate theories. The important results obtained on the mechanism and kinetics of HCO + HCO reaction can be concluded as follows: (1) the main products of the title reaction are predicted to be CO + CO + H$_2$, HCOH + CO, *cis*-(CHO)$_2$ and *trans*-(CHO)$_{2.}$. (2) As expected, the bimolecular rate constants for the formation of *cis*-(HCO)$_2$ and *trans*-(CHO)$_2$ are strongly pressure dependent while the rate constants for the product channels CO + CO + H$_2$ and anti-HCOH + OH are slightly pressure dependent. (3) At low pressures and elevated temperatures, the formation of CO + CO + H$_2$ and anti-HCOH + OH are the dominant product channels. The present calculations reveal that formaldehyde molecules are not formed majorly and the anti-HCOH is the dominant product.

REFERENCES

[1]   Warnatz, J.; Maas, U.; Dibbl, R. W., Combustion: Physical and Chemical Fundamentals, Modeling and Simulation, Experiments, Pollutant Formation. Springer-Verlag, Berlin Heidelberg, 2006.

[2]   Becerra, R.; Carpenter I. W.; Walsh, R., Time-resolved studies of the kinetics of the reactions of CHO with HI and HBr: thermochemistry of the CHO radical and the C-H bond strengths in CH$_2$O and CHO. *J. Phys. Chem. A*, **1997**, *101*, 4185-4190, DOI:

10.1021/jp970443y.

[3] Flad, J. E.; Brown, S. S.; Burkholder, J. B.; Stark H.; Ravishankara, A. R., Absorption cross sections for the $\widetilde{A}\,^2$A" $(0,9^0,0) \leftarrow \widetilde{X}\,^2$A' $(0,0^1,0)$ band of the HCO radical. *Phys. Chem. Chem. Phys.,* **2006**, *8*, 3636-3642, DOI: 10.1039/b607185f.

[4] Reilly, J. P.; Clark, J. H.; Moore C. B.; Pimentel, G. C., HCO production, vibrational relaxation, chemical kinetics, and spectroscopy following laser photolysis of formaldehyde. *J. Chem. Phys.,* **1978**, *69*, 4381-4394, DOI: 10.1063/1.436449.

[5] Ndengué, S. A.; Dawes R., Guo, H., A new set of potential energy surfaces for HCO: Influence of Renner-Teller coupling on the bound and resonance vibrational states. *J. Chem. Phys.,* **2016**, *144*, 244301:1-9, DOI: 10.1063/1.4954374.

[6] Krasnoperova, L. N.; Chesnokov, E. N.; Stark H.; Ravishankara, A. R., Elementary reactions of formyl (HCO) radical studied by laser photolysis-transient absorption spectroscopy. *Proc. Combust. Inst.,* **2005**, *30*, 935-943, DOI:10.1016/j.proci.2004.08.223.

[7] Friedrichs, G.; Herbon, J. T.; Davidson D. F.; Hanson, R. K., Quantitative detection of HCO behind shock waves: The thermal decomposition of HCO. *Phys. Chem. Chem. Phys.*, **2002**, *4*, 5778-5788, DOI: 10.1039/b205692e.

[8] Krasnoperov, L. N.; Chesnokov, E. N.; Stark H.; Ravishankara, A. R., Unimolecular dissociation of formyl radical, HCO → H + CO, studied over 1-100 bar pressure range. J. *Phys. Chem. A*, **2004**, *108*, 11526-11536, DOI: 10.1021/jp0403994.

[9] Dammeier, J.; Colberg M.; Friedrichs, G., Wide temperature range (T = 295 K and 770-1305 K) study of the kinetics of the reactions HCO + NO and HCO + NO$_2$ using frequency modulation spectroscopy. *Phys. Chem. Chem. Phys.,* **2007**, *9*, 4177-4188, DOI: 10.1039/b704197g.

[10] Quee M. J. Y.; Thynne, J. C. J., The photolysis of organic esters. *Ber. Bunsenges. Phys. Chem.,* **1968**, *72*, 211-217, DOI: 10.1002/bbpc.19680720225.

[11] Forgeteg, S.; Berces T.; Dobe, S., The kinetics and mechanism of n-butyraldehyde photolysis in the vapor phase at 313 nm. *Int. J. Chem. Kinet.,* 1979, *11*, 219-237, DOI: 10.1002/kin.550110302.

[12] Sarkisov, O. M.; Cheskis, S. G.; Nadtochenko, V. A.; Sviridenkov E. A.; Vedeneev, V. I., Spectroscopic study of elementary reactions involving HCO, NH$_2$ and HNO. *Arch. Combust.,* **1984**, *4*, 111-120.

[13] Veyret, B.; Roussel P.; Lesclaux, R., Absolute rate constant for the disproportionation reaction of formyl radicals from 295 to 475 K. *Chem. Phys. Lett.,* **1984**, *103*, 389-392, DOI: 10.1016/0009-2614(84)80326-7.

[14] Baggott, J. E.; Frey, H. M.; Lightfoot P. D.; Walsh, R., The absorption cross section of the HCO radical at 614.59nm and the rate constant for HCO + HCO = H$_2$CO + CO. *Chem. Phys. Lett.,* **1986**, *132*, 225-230, DOI: 10.1016/0009-2614(86)80112-9.

[15] Stoeckel, F.; Schuh, M. D.; Goldstein N.; Atkinson, G. H., Time-resolved intracavity laser spectroscopy: 266 nm photodissociation of acetaldehyde vapor to form HCO. *Chem. Phys.,* **1985**, *95*, 135-144, DOI: 10.1016/0301-0104(85)80154-3.

[16] Nadtochenko, V. A.; Sarkisov O. M.; Vedeneev, V. I., Study of the reactions of the HCO radical by the intraresonator laser spectroscopy method during the Pulse photolysis of acetaldehyde. *Bull. Acad. Sci. USSR Div. Chem. Sci. (Engl. Transl.),* **1979**, *28*, 605-607, DOI: 10.1007/bf00924848.

[17] Hochanadel, C. J.; Sworski T. J.; Ogren, P. J., Ultraviolet Spectrum and reaction kinetics of the formyl radical. *J. Phys. Chem.,* **1980**, *84*, 231-235, DOI: 10.1021/j100440a001.

[18] Mulenko, S. A., Investigation of the recombination of the HCO radical in an atmosphere of argon and helium by the method of internal resonator laser spectroscopy. *J. Appl. Spectros. (Engl. Transl.),* **1980**, *33*, 35-42, DOI: 10.1007/bf00627490.

[19] Temps, F.; Wagner, H. G., Kinetics of the reactions of HCO with HCO and O$_2$. *Ber. Bunsenges. Phys. Chem.,* **1984**, *88*, 410-414, DOI: 10.1002/ bbpc.19840880418.

[20] Zhao, Y.; Schultz, N. E.; Truhlar, D. G., Exchange-correlation functional with broad accuracy for metallic and nonmetallic compounds, kinetics, and noncovalent interactions. *J. Chem. Phys.,* **2005**, *123*, 161103, 1-4. DOI: 10.1063/1.2126975.

[21] Lynch, B. J.; Zhao, Y.; Truhlar, D. G., Effectiveness of diffuse basis functions for calculating relative

energies by density functional theory. *J. Phys. Chem. A,* **2003**, *107*, 1384-1388, DOI: 10.1021/jp021590l.

[22] Raghavachari, K.; Trucks, G. W.; Pople, J. A.; Head-Gordon, M., A fifth-order perturbation comparison of electron correlation theories. *Chem. Phys. Lett.,* **1989**, *157*, 479-483, DOI: 10.1016/S0009-2614(89)87395-6.

[23] Kendall, R. A.; Dunning, T. H.; Harrison, R. J., Electron affinities of the first-row atoms revisited. Systematic basis sets and wave functions, Electron affinities of the first-row atoms revisited. Systematic basis sets and wave functions. *J. Chem. Phys.,* **1992**, 96, 6796-6806, DOI: 10.1063/1.462569.

[24] Piecuch P.; Włoch, M., Renormalized coupled-cluster methods exploiting left eigenstates of the similarity-transformed Hamiltonian. *J. Chem. Phys.,* **2005**, *123*, 224105/1-10, DOI: 10.1063/1.2137318.

[25] Włoch, M.; Gour J. R.; Piecuch, P., Extension of the renormalized coupled-cluster methods exploiting left eigenstates of the similarity-transformed hamiltonian to open-shell systems: A benchmark study. *J. Phys. Chem. A,* **2007**, *111*, 11359-11382, DOI: 10.1021/jp072535l.

[26] Song, Y. Z.; Kinal, A.; Caridade, P. J. S. B.; Piecuch P.; Varandas, A. J. C., A comparison of single-reference coupled-cluster and multi-reference configuration interaction methods for representative cuts of the H2S(1A′) potential energy surface. *J. Mol. Struct. Theochem.,* **2008**, *859*, 22-29, DOI: 10.1016/j.theochem.2008.02.028.

[27] Gaussian 09, Revision A.1, Frisch, M. J.; Trucks, G. W.; Schlegel, H. B.; Scuseria, G. E.; Robb, M. A.; Cheeseman, J. R.; Scalmani, G.; Barone, V.; Mennucci, B.; Petersson, G. A.; Nakatsuji, H.; Caricato, M.; Li, X.; Hratchian, H. P.; Izmaylov, A. F.; Bloino, J.; Zheng, G.; Sonnenberg, J. L.; Hada, M.; Ehara, M.; Toyota, K.; Fukuda, R.; Hasegawa, J.; Ishida, M.; Nakajima, T.; Honda, Y.; Kitao, O.; Nakai, H.; Vreven, T.; Montgomery, J. A., Jr.; Peralta, J. E.; Ogliaro, F.; Bearpark, M.; Heyd, J. J.; Brothers, E.; Kudin, K. N.; Staroverov, V. N.; Kobayashi, R.; Normand, J.; Raghavachari, K.; Rendell, A.; Burant, J. C.; Iyengar, S. S.; Tomasi, J.; Cossi, M.; Rega, N.; Millam, J. M.; Klene, M.; Knox, J. E.; Cross, J. B.; Bakken, V.; Adamo, C.; Jaramillo, J.; Gomperts, R.; Stratmann, R. E.; Yazyev, O.; Austin, A. J.; Cammi, R.; Pomelli, C.; Ochterski, J. W.; Martin, R. L.; Morokuma, K.; Zakrzewski, V. G.; Voth, G. A.; Salvador, P.; Dannenberg, J. J.; Dapprich, S.; Daniels, A. D.; Farkas, Ö.; Foresman, J. B.; Ortiz, J. V.; Cioslowski, J.; Fox, D. J. Gaussian, Inc., Wallingford CT, 2009.

[28] Schmidt, M. W.; Baldridge, K. K.; Boatz, J. A.; Elbert, S. T.; Gordon, M. S.; Jensen, J. H.; Koseki, S.; Matsunaga, N.; Nguyen, K. A.; Su, S. J.; Windus, T. L.; Dupuis M.; Montgomery, J. A., General atomic and molecular electronic structure system. *J. Comput. Chem.,* **1993**, *14*, 1347-1363, DOI: 10.1002/jcc.540141112.

[29] Gordon M. S.; Schmidt, M. W., Advances in electronic structure theory: GAMESS a decade later, Chap. 41, pp. 1167-1189, In theory and applications of computational chemistry, the first forty years, in: Dykstra, C. E.; Frenking, G.; Kim K. S.; Scuseria, G. E. (Eds.), Elsevier. Amsterdam, 2005.

[30] http://www.msg.chem.iastate.edu/GAMESS/GAMESS.html.

[31] Holbrook, K. A.; Pilling, M. J.; Robertson, S. H., Unimolecular Reactions. Wiley, Chichester, 1996.

[32] Gilbert, R. G.; Smith, S. C., Theory of Unimolecular and Recombination Reactions. Blackwell Scientific, Oxford, 1990.

[33] Klippenstein, S. J.; Implementation of RRKM theory for highly flexible transition states with a bond length as the reaction coordinate. *Chem. Phys. Lett.,* **1990**, *170*, 71-77, DOI: 10.1016/0009-2614(90)87092-6.

[34] Klippenstein, S. J., An efficient procedure for evaluating the number of available states within a variably defined reaction coordinate framework. *J. Phys. Chem.,* **1994**, *98*, 11459-11464, DOI: 10.1021/j100095a032.

[35] Wardlaw, D. M.; Marcus, R. A., Unimolecular reaction rate theory for transition states of any looseness. 3. application to methyl radical recombination. *J. Phys. Chem.,* **1986**, *90*, 5383-5393, DOI: 10.1021/j100412a098.

[36] Wardlaw, D. M.; Marcus, R. A., RRKM reaction rate theory for transition states of any looseness. *Chem. Phys. Lett.,* **1984**, *110*, 230-234, DOI: 10.1016/0009-

2614(84)85219-7.

[37] Klippenstein, S. J.; Khundkar, L. R.; Zewail, A. H.; Marcus, R. A., Application of unimolecular reaction rate theory for highly flexible transition states to the dissociation of NCNO into NC and NO. *J. Chem. Phys.,* **1988**, *89*, 4761-4770, DOI: 10.1063/1.455670.

[38] Klippenstein, S. J.; Wagner, A. F.; Dunbar, R. C.; Wardlaw, D. M.; Robertson, S. H., VARIFLEX: VERSION. 1.00, 1999.

[39] Hernandez, R.; Miller, W. H., Semiclassical transition state theory. A new perspective. *Chem. Phys. Lett.* **1993**, *214*, 129-136, DOI: 10.1016/0009-2614(93)90071-8.

[40] Nguyen, T. L.; Stanton J. F.; Barker, J. R., *Ab initio* reaction rate constants computed using semiclassical transition-state theory: HO + H_2 → H_2O + H and Isotopologues. *J. Phys. Chem. A* **2011**, *115*, 5118-5126, DOI: 10.1021/jp2022743.

[41] Nguyen, T. L.; Stanton J. F.; Barker, J. R., A practical implementation of semi-classical transition state

theory for polyatomics. *Chem. Phys. Lett.* **2010**, *499*, 9-15, DOI: 10.1016/j.cplett.2010.09.015.

[42] Basire, M.; Parneix P.; Calvo, F. J., Quantum anharmonic densities of states using the wang-landau method. *J. Chem. Phys.* **2008**, *129*, 081101, DOI: 10.1063/1.2965905.

[43] Wang, F.; Landau, D. P., Efficient, Multiple-Range Random-Walk Algorithm to Calculate the Density of States. *Phys. Rev. Lett.* **2001**, *86*, 2050-2053, DOI: 10.1103/PhysRevLett.86.2050.

[44] Barker, J. R.; Ortiz, N. F.; Preses, J. M.; Lohr, L. L.; Maranzana, A.; Stimac, P. J.; Nguyen, T. L.; Kumar, T. J. D., MultiWell-2016 Software; Barker, J. R., Ed.; University of Michigan: Ann Arbor, Michigan, U.S.A., 2016; http://aoss.engin.umich.edu/multiwell/.

[45] Gonzalez C.; Schlegel, H. B., Reaction path following in mass-weighted internal coordinates. *J. Phys. Chem.,* **1990**, *94*, 5523-5527, DOI: 10.1021/j100377a021.